

# Macroscopic quantum mechanics experiments

Autor(en): **Devoret, Michel H. / Martinis, John M. / Esteve, Daniel**

Objektyp: **Article**

Zeitschrift: **Helvetica Physica Acta**

Band (Jahr): **61 (1988)**

Heft 5

PDF erstellt am: **05.08.2024**

Persistenter Link: <https://doi.org/10.5169/seals-115966>

## **Nutzungsbedingungen**

Die ETH-Bibliothek ist Anbieterin der digitalisierten Zeitschriften. Sie besitzt keine Urheberrechte an den Inhalten der Zeitschriften. Die Rechte liegen in der Regel bei den Herausgebern.

Die auf der Plattform e-periodica veröffentlichten Dokumente stehen für nicht-kommerzielle Zwecke in Lehre und Forschung sowie für die private Nutzung frei zur Verfügung. Einzelne Dateien oder Ausdrucke aus diesem Angebot können zusammen mit diesen Nutzungsbedingungen und den korrekten Herkunftsbezeichnungen weitergegeben werden.

Das Veröffentlichen von Bildern in Print- und Online-Publikationen ist nur mit vorheriger Genehmigung der Rechteinhaber erlaubt. Die systematische Speicherung von Teilen des elektronischen Angebots auf anderen Servern bedarf ebenfalls des schriftlichen Einverständnisses der Rechteinhaber.

## **Haftungsausschluss**

Alle Angaben erfolgen ohne Gewähr für Vollständigkeit oder Richtigkeit. Es wird keine Haftung übernommen für Schäden durch die Verwendung von Informationen aus diesem Online-Angebot oder durch das Fehlen von Informationen. Dies gilt auch für Inhalte Dritter, die über dieses Angebot zugänglich sind.

# Macroscopic quantum mechanics experiments

By Michel H. Devoret,<sup>1)</sup> John M. Martinis<sup>1)</sup> and Daniel Esteve

Service de Physique du Solide et de Resonance Magnetique, CEN Saclay, 91191 Gif-sur-Yvette Cedex, France

and John Clarke

Physics Department, University of California, Berkeley and Materials and Chemical Sciences Division, Lawrence Berkeley Laboratory, Berkeley, CA 94720, USA

(22. II. 1988)

## 1. Introduction

Do the laws of Quantum Mechanics apply to macroscopic degrees of freedom? Until very recently this had not been tested experimentally, even though the words ‘macroscopic quantum effects’ are used in the literature to describe phenomena like superfluidity or superconductivity. As Leggett has emphasized [1], there are two classes of macroscopic quantum effects. In the first class, to which belong superfluidity and superconductivity, are quantum phenomena affecting only microscopic variables but that add coherently on a macroscopic scale. In the second class are quantum effects displayed directly by a macroscopic variable. A comparison involving a single crystal may help to clarify this point: the discrete orientations of the faces of the crystal are manifestations of the underlying quantum atomic structure revealed on a macroscopic scale by the coherent stacking of atoms. This is an example belonging to the first class of macroscopic quantum effects. On the other hand, an hypothetical observation of the rotation of the crystal as a whole due to zero-point motion would be a macroscopic quantum effect of the second class. The actual observation of phenomena belonging to this second class is the subject of this lecture.

Because Planck’s constant is so small, the quantum behavior of a macroscopic degree of freedom is usually unobservable. The above single crystal, even if of the size of a speck of dust, will normally move spontaneously only by Brownian motion which is a purely classical phenomenon. However, electronic systems have the potential for displaying genuine macroscopic quantum effects. Let us consider the simple circuit consisting of an inductor  $L$  connected across a

---

<sup>1)</sup> MHD and JMM were part of J. Clarke’s group in Berkeley at the time the experiments presented in this paper were performed.

capacitor  $C$ . Observations on this oscillator are made via leads which can be modelled as an infinitely long transmission line of characteristic impedance  $Z_c$ . The flux  $\varphi$  in the inductor is the macroscopic degree of freedom of the system, its conjugate momentum being the charge  $q$  on the capacitor. The natural angular frequency of oscillation is  $\omega_0 = (LC)^{-1/2}$  and the impedance on resonance is  $Z_0 = (L/C)^{1/2}$ . The quality factor of the oscillator is  $Q = Z_c/Z_0$ . To observe quantum effects two criteria need to be satisfied: (i) The lifetimes of the quantum states of the macroscopic degree of freedom must be long on its characteristic time scale. This is equivalent to the condition  $Q \gg 1$ . (ii) The thermal energy must be small compared with the separation of the quantized energy levels. This is expressed by  $\hbar\omega_0 \ll k_B T$  where  $T$  is the temperature of the source of damping, here the system of leads. These constraints are satisfied for  $L = 350$  pH and  $C = 15$  pF provided that  $T = 10$  mK and  $Z_c = 50 \Omega$ . The natural frequency of the oscillator is then  $\omega_0/2\pi = 2$  GHz. These conditions can nowadays be realized and controlled routinely in the laboratory. Thus for this system one can hope to challenge the smallness of  $\hbar$ .

Unfortunately the harmonic oscillator is a system that does not display quantum effects easily because it is always in the correspondance limit. The average values of the position or the momentum follow classical equations of motion. Quantum Mechanics is revealed in higher moments like the variances of the basic variables but these higher moments are very hard to measure. For our  $LC$  oscillator, we have for example  $\langle q^2 \rangle \approx 10^{-35} C^2 \approx (20e)^2$ . Also, there is a more fundamental objection to the use of a linear system to look for macroscopic quantum effects since in that case the distinction between effects resulting from the coherent addition of microscopic variables and genuine macroscopic quantum effects is harder to draw [1].

One is thus led to use a non-linear oscillator involving a Josephson tunnel junction. This component is a sandwich of two superconductors separated by a thin oxide layer. In contrast with other non-linear electronic devices, it remains active at the very low temperatures required by the search for quantum effects. The macroscopic variable that describes the state of the junction is the phase difference  $\delta$  between the condensates of Cooper pairs in the superconductors on either side of the tunnel barrier. Let us discuss in some detail the nature of the variable  $\delta$  since it is crucial to the meaning of the macroscopic quantum mechanical experiments.

At the low temperatures where the experiments are performed, all internal electronic degrees of freedom of the superconductors are in their ground states and, *a priori*, the variables of the junction are the phase differences of the Cooper pairs that tunnel across the barrier. But the rigidity of the superconductive ordering forces all the tunneling pairs to have the same phase  $\delta$ . The variable  $\delta$  thus describes the collective motion of the tunneling pairs and is the single remaining degree of freedom of the junction. Note that this rigidity of the condensates and thereby the existence of  $\delta$  are themselves a macroscopic quantum effect of the first class. Returning to the comparison with a crystal, it appears that the rigidity of the condensates is similar to the interatomic forces

that hold the crystal together and whose details are irrelevant to the predictions of the motion of the crystal as a whole. For these predictions, only macroscopic parameters like moments of inertia need to be known because all internal degrees of freedom are, so to speak, 'frozen out'.

The question is now whether the macroscopic variable  $\delta$  can itself behave quantum-mechanically. We performed at Berkeley a series of experiments [2] that demonstrate that indeed it does. Since the experiments have been described in details elsewhere [2], we will sketch here only their general principles.

First, what do we mean when we say we observe experimentally the quantum behavior of a system? For a microscopic system like an atom the situation is simple. The properties of each particle (electrons and nucleus) are known independently and the dynamical equations of the system can be obtained from first principles. To make predictions one has to solve these equations within a certain theoretical framework: classical, quantum mechanical, etc. . . Of course, for the atom the quantum predictions are the only ones that correspond to the observations. As for a macroscopic system, whose complete description can never be obtained in every detail, the situation is more complicated and involves a two-step procedure. In the first step one measures the time evolution of the system in a regime where thermal fluctuations are large compared with the expected quantum fluctuations. One obtains thereby the parameters entering in the classical equations of motion that characterize the macroscopic variables of the system. In the second step, the thermal fluctuations are reduced well under the level of the expected quantum fluctuations. Also, one makes sure that all other parasitic noise that could mimick quantum fluctuations is eliminated. The new time evolution is then measured. Finally one compares the results obtained in the second step with the predictions of the quantum theory based on the parameters measured 'classically' in the first step. If they agree, the quantum behavior of the macroscopic system is said to have been observed.

In pioneering experiments [3, 4, 5, 6] on macroscopic quantum tunneling (a phenomenon that will be described later) involving Josephson junctions, the temperature of the junctions was lowered to that quantum fluctuations were expected to dominate. The results of these experiments were consistent with a quantum mechanical interpretation of the behavior of the phase difference of the junctions. Recently, more sophisticated experiments investigated the question of the influence of dissipation on tunneling [7, 8] which had been calculated theoretically [1, 9].

However, a persistent difficulty in all these experiments has been the correct determination of the parameters of the principal component of the macroscopic system, namely the Josephson junction. Without a precise knowledge of these parameters no quantitative comparison with quantum theories can be made. In the early experiments, some of the important parameters were treated as adjustable parameters in the predictions or were estimated from measurements of properties not directly connected to the dynamical properties involved in the tunnelling experiment. In the experiment of Schwartz *et al.* [8] separate measurements of the relevant parameters are made but they are based partially

on a quantum analysis of the raw experimental data. This is why we devised new experimental techniques to ensure that all the parameters of the junction would be measured *in situ* using *classical* phenomena, in particular under conditions that guarantee that no spurious noise reaches the junction.

In the following the emphasis will be put on the particular procedures we used to solve the two problems of noise shielding and parameter determination. Before discussing these central issues, we begin with a short description of the classical dynamics of our macroscopic system: a Josephson junction biased with a constant current.

## 2. Classical dynamics of the current biased Josephson junction

As we have seen, for the purpose of understanding our experiment, the underlying physics of the superconductors and their coupling through the oxide barrier can be safely ignored and the junction can be thought of as an ideal *non-linear* inductor in parallel with a capacitor (see Fig. 1). An ideal linear inductor would be a simple coil made of superconducting wire and would be characterized by an energy quadratic in the flux through the coil. Instead, the ideal non-linear inductor that constitutes a Josephson junction has an energy given by:

$$E = -I_0(\phi_0/2\pi) \cos \delta \tag{1}$$

where  $\phi_0$  is the flux quantum. The variable  $\delta$  is the phase difference across the junction. The quantity  $\varphi = (\phi_0/2\pi)\delta$  is analogous to the flux through the linear inductor in the sense that the current and voltage for the non-linear element satisfy also  $i = dE/d\varphi$  and  $v = d\varphi/dt$ . For small  $\delta$ , the non-linear inductor of the junction behaves as an effective inductor:  $\varphi = L_{\text{eff}}i$  with  $L_{\text{eff}} = \phi_0/2\pi I_0$ .

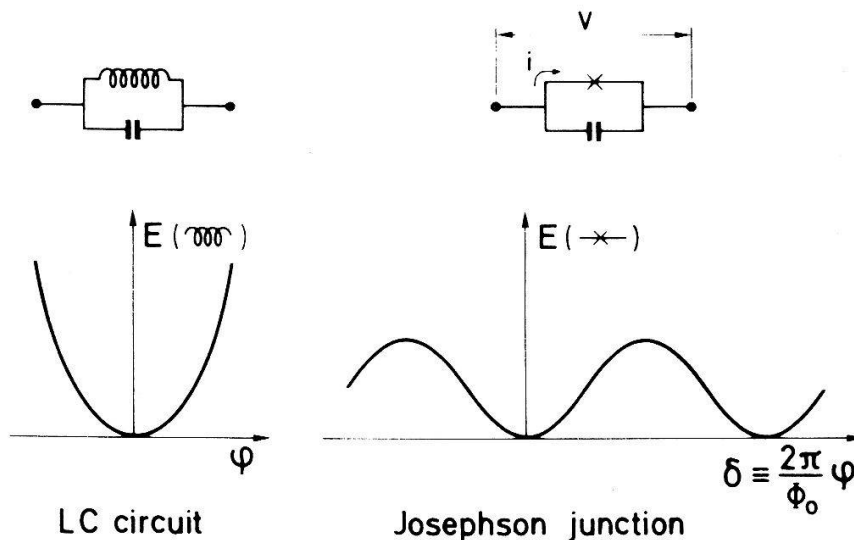


Figure 1  
Comparison between a Josephson junction, which consists of a non-linear inductor in parallel with a capacitor, and a linear LC circuit.



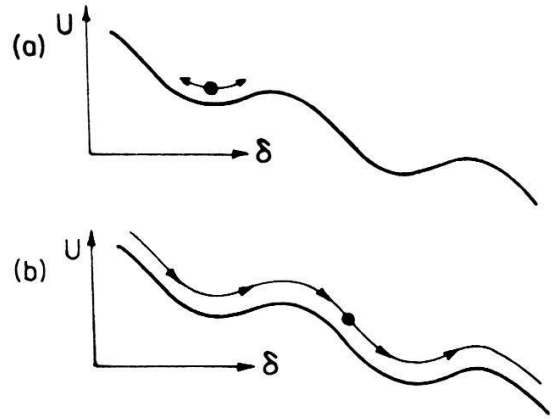


Figure 2  
The two states of a Josephson junction biased with a current  $I < I_0$ ; a)  $\langle \dot{\delta} \rangle = 0$  (zero voltage state); b)  $\langle \dot{\delta} \rangle \neq 0$  (voltage state)

The junction by is thus characterized by two parameters: the critical current  $I_0$  and the capacitance  $C$ . We will see that the coupling of the junction to the measuring apparatus involves additional parameters.

When it is biased with a constant current  $I$ , the junction is equivalent to the model of a particle moving in a tilted washboard potential (see Fig. 2). The mass of the particle is the capacitance  $C$ . The tilt of the washboard is the ratio  $I/I_0$ . When  $I < I_0$  the potential has relative minima and the particle can be in two states. In the so-called zero voltage state the particle is confined in one well (see Fig. 2a). The average velocity and hence the average voltage across the junction is zero. In the other state, called the voltage state, the particle runs down the washboard at an average constant velocity determined by frictional forces (see Fig. 2b). In our experiment the velocity is limited solely by the breaking of Cooper pairs in the superconductors and corresponds to the gap voltage which is of the order of 2 mV.

The zero voltage state is metastable and eventually decays into the voltage state. It is easy to determine the decay rate of the zero voltage state by monitoring the voltage across the junction. The experiment is performed as follows: initially  $I = 0$  and the particle representing the phase difference is in a relative minimum of the washboard potential. We ramp the bias current from 0 to  $I < I_0$ , and wait until a voltage appears across the junction. This voltage is the signature that the particle has escaped from the well and accelerated down the washboard potential. It is worth noting that the acceleration of the particle 'amplifies' the very small voltage pulse associated with the escape event. This built-in amplification process is a particularly attractive feature of the current biased junction.

Because the acceleration process is so fast, the time at which the voltage is measured across the junction can be taken as the time at which the particle escapes. We repeat the experiment a large number of times to obtain the average escape rate.

By measuring the escape rate as a function of the bias current which controls the shape and the size of the potential well one gains access to some aspects of the behavior of the particle inside the well. However, to obtain a complete picture of the motion of the particle one needs extra 'knobs' on the experiment. This is where our experiments differ fundamentally from all the others: we add to

the current bias a weakly perturbing microwave current and measure the *change* in the escape rate induced by this perturbation. The dependence of this change on the frequency and bias current provide additional information that, when combined with the first measurement, enable us to reconstruct the *dynamics* of the particle in the well.

We have supposed up to now that the current source and the voltmeter are ideal. In practice they have always some finite impedance in parallel with them, in particular the impedance due to the electromagnetic coupling between the leads connecting the instruments to the junction. Even though these impedances may be negligible at low frequencies and may not affect a quasi-static measurement such as an  $I-V$  characteristic, they become of prime importance at the frequencies relevant for the motion of the particle in the well, which are in the microwave range. The junction will thus see an effective admittance in parallel with it.

As we will see in the next section, it is possible to arrange the circuit so that this admittance behaves essentially like a resistor in parallel with a capacitor. This picture is valid in a broad frequency range around the characteristic frequency of the particle in the well. The effect of the external shunting capacitances is simply to renormalize the capacitance of the junction. The effect of the resistance is two-fold. One effect is to damp the motion of the particle in the well. The other is to act as a thermal bath and to induce fluctuations in the motion of the particle. Two additional parameters must then be introduced to take into account the coupling of the junction with the measuring apparatus: the resistor  $R$  and its temperature  $T$ . The temperature of the junction itself is unimportant as long as its intrinsic damping is negligible when compared with the damping provided by the external resistor  $R$  – this is always the case in our experiment.

The above description of our current biased Josephson junction corresponds to the circuit of Fig. 3 and leads to the following classical equation of motion:

$$C((\phi_0/2\pi)^2) \ddot{\delta} + R^{-1}(\phi_0/2\pi)^2 \dot{\delta} + \frac{\partial}{\partial \delta} U(\delta) = (\phi_0/2\pi)I_N(t), \tag{2}$$

where  $U(\delta)$  is the tilted cosine potential:

$$U(\delta) = (-I_0\phi_0/2\pi)[\cos \delta + (I/I_0)\delta], \tag{3}$$

and where the current noise  $I_N$  satisfies:

$$\int_{-\infty}^{+\infty} \langle I_N(t)I_N(0) \rangle_T e^{i2\pi\nu t} dt = \frac{2k_B T}{R}. \tag{4}$$

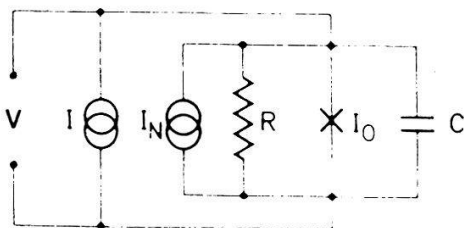


Figure 3  
Equivalent circuit for our junction coupled to its measurement apparatus which has a finite impedance at microwave frequencies. The resistor  $R$  models the real part of this impedance. The capacitor  $C$  includes a contribution from the imaginary part of the impedance.

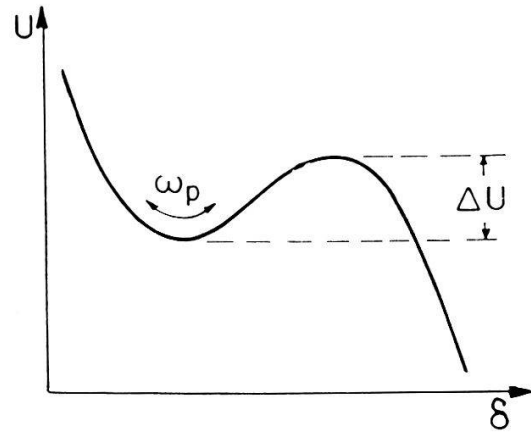


Figure 4  
Cubic potential from which the particle representing the junction phase difference escapes.

In practice the bias current  $I$  is very close to the critical current and hence the potential from which the particle escapes is very nearly cubic (see Fig. 4). The barrier height  $\Delta U$  and the oscillation frequency  $\omega_p/2\pi$  at the bottom of the well (plasma frequency) are two useful independent parameters that completely describe the potential and are given, to a very good approximation, by:

$$\Delta U = (2\sqrt{2} I_0 \phi_0 / 3\pi)(1 - I/I_0)^{3/2} \quad (5)$$

and:

$$\omega_p = (\sqrt{2} 2\pi I_0 / \phi_0 C)^{1/2}(1 - I/I_0)^{1/4}. \quad (6)$$

The damping due to the resistor is conveniently described by the dimensionless quality factor of the small oscillations at the bottom of the well:

$$Q = RC\omega_p. \quad (7)$$

Before turning to the problem of determining the parameters  $I_0$ ,  $C$ ,  $R$  and  $T$ , we will describe some crucial features of our apparatus, namely the filters that isolate the junction from unwanted noise from the measurement circuitry.

### 3. Decoupling the junction from ambient noise

It goes without saying that the junction must be completely shielded from parasitic electromagnetic sources like radio stations. But this is far from being sufficient. Thermal current noise from the measuring apparatus at room temperature – i.e. the current source and the voltage amplifier – must also be prevented from reaching the junction through its leads. This is achieved by interposing a series of filters between the junction and the measuring apparatus. These filters screen out all frequencies except a very narrow range near zero so that we are still able to vary the bias current and detect the voltage rise as the junction switches to the voltage state. The range is chosen to be sufficiently narrow that noise in that frequency band is negligible and sufficiently wide that a good time resolution of the lifetime of the zero voltage state is achieved.



In practice such a low pass wideband filter can be made conveniently only with filter elements having substantial dissipation. Because of this dissipation, the filter itself will produce noise and each filter in the chain must be at a lower temperature than the preceding one. In view of the stringent filtering requirements of the experiment, we developed a special type of filter. It consists of a spiral coil of insulated wire inside a copper tube filled with copper powder with a grain size of about  $30\ \mu\text{m}$ . Since each grain is insulated from its neighbour by an oxide layer, the effective area of the copper is enormous and thus provides substantial skin effect losses even at the lowest temperatures. The lowest part of the radio-frequency spectrum was dealt with by a classic RC network. The chain of filters provided a total attenuation of more than 200 dB.

The last filter was carefully engineered since it imposes the damping and hence the fluctuations of the phase difference of the junction. It consists of an attenuating coaxial line that also relies on copper powder for the source of damping. The copper powder is thermalized by epoxy which is injected between the grains. The junction is mounted as closely as possible to the end of the line to ensure that the impedance discontinuity between the junction and the line occurs on a distance small compared with the wavelength at the plasma frequency. This microwave engineering ensured that the impedance seen by the junction behaved essentially as a parallel RC combination with no important spurious resonances.

#### **4. Determination of junction parameters using classical phenomena**

##### *4.1. Capacitance and resistance*

The parameters  $\omega_p$  and  $Q$  were determined by resonant activation. This phenomenon involves the enhancement of the escape by a microwave irradiation of the junction. This enhancement is determined by taking the ratio of the escape rate measured in the presence of microwave irradiation of power  $P$  and of the escape rate measured under the same conditions but without microwaves. Below the plasma frequency, the enhancement is a smoothly increasing function of the microwave frequency. But when a frequency just slightly below the plasma frequency is reached, the enhancement drops steeply to zero. As numerical simulations [10, 11] and analytical calculations [12, 13, 14] have shown, the plasma frequency is given, apart from a small correction, by that frequency at which the enhancement drops steeply, while  $Q$  is given by the range of frequency over which the drop occurs. Experimentally, it is easier to keep the irradiation frequency fixed and to vary the plasma frequency by varying the bias current (see Eq. (6)). An example is shown in Fig. 5. At the resonant current  $I_{\text{res}}$ , the plasma frequency is equal to the applied microwave frequency. From equation (6) we can deduce the plasma frequency at other values of the bias current. The value of  $Q$  can be inferred from the width in current of the *rf* roll-off of the enhancement.

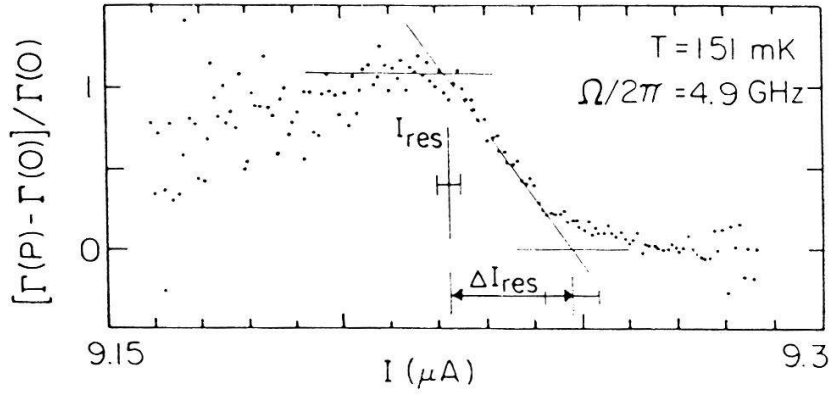


Figure 5  
Microwave induced enhancement of the escape rate measured as a function of the bias current.  $\Omega/2\pi$  is the irradiation frequency.

#### 4.2. Critical current and temperature

In the thermal regime the escape of the particle from the well occurs by thermal activation. The rate is given by [15]:

$$\Gamma_t = a_t (\omega_p/2\pi) \exp(-\Delta U/k_B T), \tag{8}$$

where the prefactor  $a_t$  is given by:

$$a_t = 4/[(1 + Qk_B T/1.8 \Delta U)^{1/2} + 1]^2. \tag{9}$$

We determine  $I_0$  and  $T$  from the dependence of the escape rate on the bias current. As is evident from equation (5) and equation (8) a plot of the experimentally determined quantity  $\{\ln[\omega_p(I)/2\pi\Gamma(I)]\}^{2/3}$  vs.  $I$  should, neglecting departures of  $a_t$  from unity, be a straight line with slope scaling as  $T^{-2/3}$  that intersects the current axis at  $I_0$ . Figure 6 shows the three examples of such plots. As expected the dashed lines drawn through the data intersect the current axis at very nearly the same point. Taking into account the correction due to the

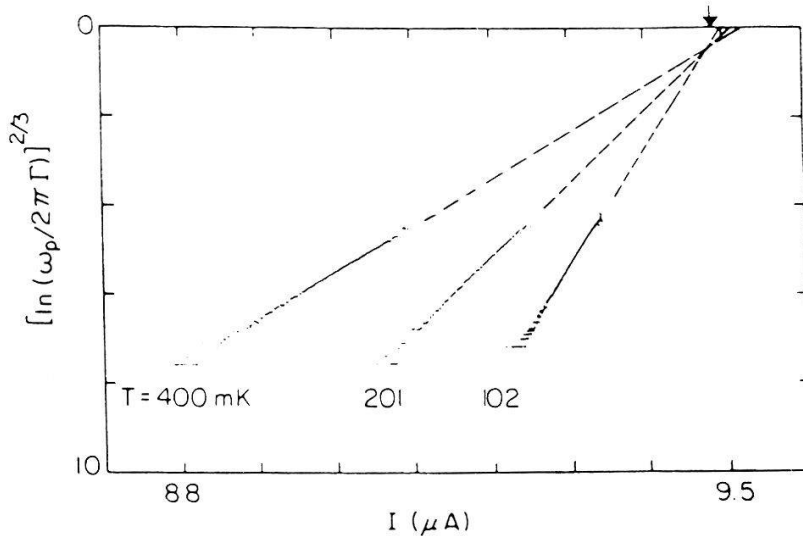


Figure 6  
Plot of the  $2/3$  power of the logarithm of the escape rate vs. bias current. On this plot, data should fall on a straight line. Dashed lines are least-square fits to the data. The arrow indicates the value of the critical current.

departure of  $a_i$  from unity we obtain a temperature independent value of the critical current (arrow on Fig. 6). We find excellent agreement between the temperature measured from the current dependence of the escape rate and the temperature measured by our thermometers. The fact that the data indeed fall on a straight line is also an additional check that the escape occurs through thermal activation at a well defined temperature.

We have described how we obtain all the system parameters using the properties of the escape in the classical regime. We will now describe the second part of the experiment performed in the quantum regime obtained by reducing the temperature and where the same properties are remeasured.

## 5. Measurements in the quantum regime

### 5.1. Quantized energy levels

At low temperatures, one has to decrease substantially the barrier height to obtain a short enough lifetime of the zero voltage state. Thus, there are only a few levels in the well. For temperatures  $T$  slightly greater than  $\hbar\omega_p/2\pi k_B$  [1, 9], the escape in the absence of microwaves occurs essentially via thermal activation through these discrete states to the continuum of states above the potential barrier. In the presence of microwave power  $P$  however, the population of the excited states at the top of the well increases. The particle then escapes at a rate  $\Gamma(P)$  which is greater than  $\Gamma(P=0)$ . Consequently, one expects a resonant enhancement of the escape rate when the irradiation frequency matches a transition frequency between two energy levels. As in the classical regime, we keep the frequency fixed and vary the bias current  $I$ , thereby continuously changing all the level spacings. One can in this way determine spectroscopically the position of the energy levels in the well. Our results for a  $C = 47$  pF junction are plotted in Fig. 7a.

These results can be compared with a quantum calculation of the energy levels based on an *in situ* measurement of the parameters  $\Delta U$  and  $\omega_p$ . An unambiguous agreement between the experimental value of the relative positions of the resonances and their theoretical predictions is found (see Fig. 7b). The relatively small shift in the absolute value of the position of the resonances is due to the uncertainty in the determination of the critical current (the resulting uncertainty in the  $0 \rightarrow 1$  transition frequency is shown by the dotted line).

In this experiment, the junction is only slightly damped with a  $Q$  factor around 80. The relative width of the  $0 \rightarrow 1$  resonance in the quantum regime is approximately equal to  $1/Q$ , as predicted by theory [16].

### 5.2. Quantum tunneling

In the absence of microwaves and for temperatures below  $\hbar\omega_p/2\pi k_B$ , escape from the well occurs via quantum tunneling through the potential barrier. This

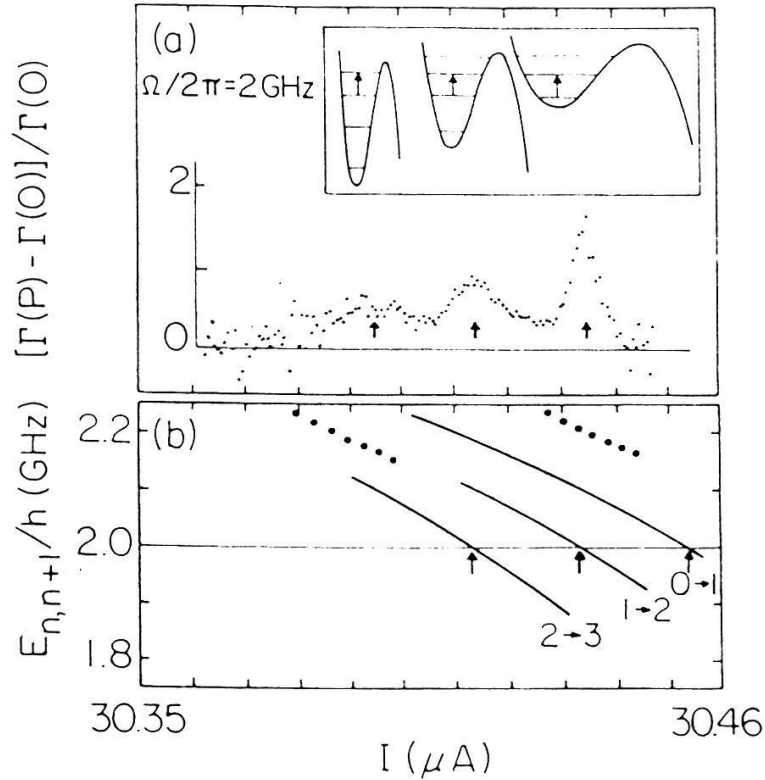


Figure 7

a) Microwave induced enhancement of the escape rate as function of bias current for  $k_B T / \hbar \omega_p = 0.29$ . Arrows indicate positions of resonances. Inset represents the corresponding transitions between energy levels. b) Calculated energy level spacings. Dotted lines indicate uncertainties in  $E_{01}$  due to errors in the determination of junction parameters. Arrows indicate values of bias current at which resonances are predicted.

process has received the name of Macroscopic Quantum Tunneling (MQT) since it affects the state of the junction as a whole and is unrelated to the tunneling of individual Copper pairs. MQT is analogous to the  $\alpha$  decay of a heavy nucleus, the detection of the  $\alpha$  particle by a counter being replaced here by the detection of a voltage across the junction. The predicted quantum tunneling rate is [1]:

$$\Gamma_q = a_q \frac{\omega_p}{2\pi} \exp \left[ -7.2 \frac{\Delta U}{\hbar \omega_p} \left( 1 + \frac{0.87}{Q} + \dots \right) \right], \quad (10)$$

where:

$$a_q = [120\pi(7.2 \Delta U / \hbar \omega_p)]^{1/2}. \quad (11)$$

Equation (10) is written so that a direct comparison with equation (8) can be made. The usual WKB result is obtained by letting  $Q \rightarrow \infty$  in equation (10).

Our results are shown in Fig. 8 where the escape rate is plotted as an escape temperature  $T_{\text{esc}}$  (defined through the relation  $\Gamma = (\omega_p/2\pi) \exp(-\Delta U/kT_{\text{esc}})$ ) versus temperature. This measurement was made on a  $C = 6$  pF junction which could be placed more firmly in the quantum regime (at the expense of a somewhat greater damping:  $Q = 30$ ; however the damping was not strong enough to affect the escape rate significantly). The open circles correspond to a measurement with a magnetic field applied to the junction to lower its critical

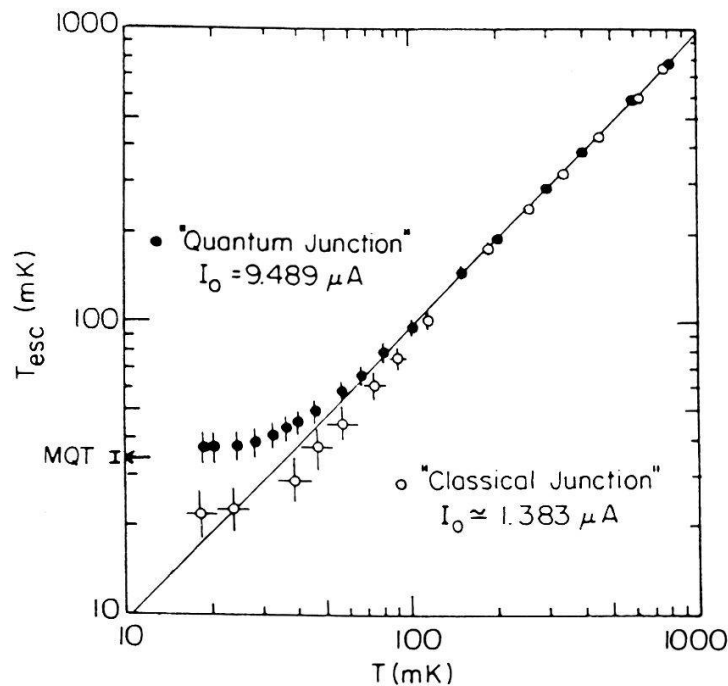


Figure 8

Escape temperature plotted against temperature for two values of the critical current. The solid line is the classical prediction  $T_{\text{esc}} = 0.95 T$  (equation (8)). The arrow is the quantum prediction (equation (10)).

current. With a reduced critical current, the plasma frequency is lower and the junction should behave classically down to the lowest temperatures. Indeed the escape rate followed the classical prediction (solid line) showing that no significant amount of external noise was reaching the junction. When the critical current was restored to its original value, we measured a higher value of the escape rate (solid dots). The escape rate became temperature independent at low temperatures, as expected if the escape mechanism is dominated by quantum fluctuations. This interpretation is supported by the quantitative agreement between this limiting value of the measured escape rate and its theoretical prediction (arrow shows the prediction of Eq. (10); we have also indicated the error bar of the prediction due to the uncertainties in the classical measurements of the parameters). We note that in our experiment the predicted effect of dissipation on tunneling is too small to be discernible.

In a recent experiment done on a junction shunted by a metallic thin film resistor [17] and for which the damping factor  $Q$  was 1.8, a reduction of about 300 of the tunneling rate from its  $Q = \infty$  value was measured. This result, well outside the uncertainties of the experiment, shows that dissipation strongly suppresses tunneling by a factor which is in very good quantitative agreement with the predictions of the quantum theory [1, 9].

## 6. Conclusion

Our measurements of the lifetime of the zero voltage state of a current biased Josephson junction agree quantitatively with predictions based on quan-



tum theory, all the relevant parameters being measured *in situ*. They show that the phase difference across a Josephson junction, a macroscopic variable, behaves quantum-mechanically. The meaning of this result is two-fold.

First, the experimental range of validity of Quantum Mechanics has been extended. We have shown that the property of Quantum Mechanics to treat all degrees of freedom on the same footing whatever the *complexity* of the system they describe remains valid even for a composite, macroscopic system like a Josephson junction. We are aware that many physicists believe Quantum Mechanics to be a fundamental theory that cannot 'break down'. Nevertheless, we hold the view that this should be checked as far as available technology permits. A further challenge in the domain of macroscopic Quantum Mechanics is, for example, the observation of Macroscopic Quantum Coherence [1].

Second, our experiment shows that it is indeed possible, given enough filters and shields, to isolate an electronic degree of freedom like a voltage or a current from its environment sufficiently well for its behavior to be entirely dominated by quantum effects. This opens a new area of research on superconducting circuits that would preform quantum signal processing such as squeezing [18] and perhaps implement the so-called back action evasion amplifiers that are needed for the detection of gravity waves [19]. Finally, the quantum electronician can dream of building exotic macroscopic 'atoms with wires' that would display new quantum phenomena with no equivalents in the microscopic world.

## Acknowledgments

We have benefited from interesting discussions with H. Grabert, A. J. Leggett, S. Reynaud and C. Urbina. This work was supported by the director, Office of Energy Research, Office of Basic Energy Sciences, Materials Sciences Division of the U.S. Department of Energy under Contract n° DE-AC03-76SF00098.

## REFERENCES

- [1] A. J. LEGGETT, Prog. Theor. Phys. (Suppl.) 69, 80 (1980); *Lecture Notes, Les Houches Summer School on Chance and Matter*, eds. J. Souletie, R. Stora and J. Vannimenus (North-Holland, Amsterdam, 1987).
- [2] J. M. MARTINIS, M. H. DEVORET and J. CLARKE, Phys. Rev. Lett. 55, 1543 (1985); M. H. DEVORET, J. M. MARTINIS and J. CLARKE, Phys. Rev. Lett. 55, 1908 (1985); J. MARTINIS, M. H. DEVORET and J. CLARKE, Phys. Rev. B 35, 4682 (1987).
- [3] W. DEN BOER and DE BRUYN OUBOTER, Physica 98B, 185 (1980).
- [4] R. J. PRANCE, A. P. LONG, T. D. CLARK, A. WIDOM, J. E. MUTTON, J. SACCO, M. W. POTTS, G. MEGALLOUDIS and F. GOODALL, Nature 289, 543 (1981).
- [5] R. F. VOSS and R. A. WEBB, Phys. Rev. Lett. 47, 265 (1981).
- [6] L. D. JACKEL, J. P. GORDON, E. L. HU, R. E. HOWARD, L. A. FETTER, D. M. TENNANT, R. W. EPWORTH and J. KURKIJARVI, Phys. Rev. Lett. 47, 697 (1981).
- [7] S. WASHBURN, R. A. WEBB, R. F. VOSS and S. M. FARIS, Phys. Rev. Lett. 54, 2712 (1985).
- [8] D. B. SCHATZ, B. SEN, C. N. ARCHIE and J. E. LUKENS, Phys. Rev. Lett. 55, 1547 (1985).
- [9] H. GRABERT, P. OLSCHOWSKI and U. WEISS, Phys. Rev. B36, 1931 (1987).
- [10] M. H. DEVORET, J. M. MARTINIS, D. ESTEVE and J. CLARKE, Phys. Rev. Lett. 53, 1260 (1984).

- [11] M. H. DEVORET, D. ESTEVE, J. M. MARTINIS, A. CLELAND and J. CLARKE *Phys. Rev. B* **36**, 58 (1987).
- [12] T. FONSECA and P. GRIGOLINI, *Phys. Rev. A* **33**, 122 (1986).
- [13] B. I. IVLEV and V. I. MEL'NIKOV (preprint).
- [14] A. I. LARKIN and YU. N. OVCHINNIKOV, *J. of Low Temp. Phys.* **63**, 317 (1986).
- [15] M. BÜTTIKER, E. P. HARRIS and R. LANDAUER, *Phys. Rev. B* **28**, 1268 (1983).
- [16] D. ESTEVE, M. H. DEVORET and J. MARTINIS, *Phys. Rev. B* **34**, 158 (1986).
- [17] A. CLELAND, J. MARTINIS and J. CLARKE, to be published in *Phys Rev. B*.
- [18] R. E. SLUSHER, L. W. HOLLBERG, B. YURKE, J. C. MERTZ and J. F. VALLEY, *Phys. Rev. Lett.* **55**, 2409 (1985).
- [19] C. M. CAVES, K. S. THORNE, R. W. P. DREVER, V. D. SANDBERG and M. ZIMMERMAN, *Rev. Mod. Phys.* **52**, 341 (1980).